



International Congress of Science and Technology of Metallurgy and Materials, SAM –
CONAMET 2014

Characterization of fatigue life of ultrafine grained NiTi superelastic wires under uniaxial loading

Sebastián Jaureguizar^{a,*}, Hugo Soul^a, Mirco Chapetti^b, Alejandro Yawny^a

^a*División Física de Metales, Centro Atómico Bariloche, Av. Bustillo 9500, S.C. Bariloche (8400), Argentina*

^b*INTEMA (CONICET-University of Mar del Plata), J. B. Justo 4302, Mar del Plata (7600), Argentina*

Abstract

The role of the stress induced martensitic transformation on the fatigue life of Ni-rich ultrafine grained NiTi superelastic wires has been investigated. Two types of experiments have been considered to elucidate the question. In the first class, the stress range was kept in between the forward and reverse plateaus levels, thus avoiding evident martensitic stress induced transformation. Strain controlled experiments were performed in wires in fully austenite, fully stress induced martensite and austenite–martensite coexistence zone with nearly half of the wire length transformed to martensite. In the second type of experiments, pseudoelastic cycling was performed. In this case the stress induced austenite to martensite transformation is involved. The obtained results indicate a definite deleterious effect of the stress induced transformation on the fatigue life. Additional important aspects related with fatigue life of NiTi wires like fretting fatigue effects in the grip–specimen contact region and the relative importance of the crack initiation and crack propagation stages on the total fatigue life are also presented.

© 2015 The Authors. Published by Elsevier Ltd. This is an open access article under the CC BY-NC-ND license (<http://creativecommons.org/licenses/by-nc-nd/4.0/>).

Peer-review under responsibility of the Scientific Committee of SAM–CONAMET 2014

Keywords: NiTi shape memory alloys; fatigue; pseudoelasticity; mean stress effect

1. Introduction

The shape memory effect and the pseudoelastic behaviour are properties that make NiTi alloys an excellent candidate for different applications ranging from endovascular stents to damping devices. Shape memory is generated by a martensitic transformation which changes a high temperature phase (B2 structure in NiTi) into a low

* Corresponding author. Tel.: +054-0294-444-5100-5290; fax: +054-0294-444-5299.

E-mail address: jaureguizar@cab.cnea.gov.ar

temperature phase (B19' structure in NiTi) in a reversible, diffusionless lattice shear process [Saburi (1998)]. The martensitic phase can form various habit plane variants which accommodate each other to reduce the elastic strains associated with the transformation. Lattice invariant shear processes like slip and twinning aid in reducing the occurring misfits. The martensitic transformation may be triggered by either a temperature change or an applied stress [Melton and Mercier (1979)]. A stress-induced transformation can easily be characterized by the critical stresses at which the forward or reverse transformation occurs during loading/unloading. The related shape change leads to plateaus in stress-strain plots of uniaxial, isothermal tests. In NiTi alloys, the transformation stresses show strong temperature dependence. Typical values are in the range of 7 MPa/K [Yawny et al. (2005)]. Mechanical cycling of NiTi alloys results in a non-even decrease of the direct transformation (more pronounced) and reverse transformation (less pronounced) stresses with a consequent decrease in hysteresis and accumulation of permanent strain [Olbricht et al. (2008)]. These changes are referred to as functional fatigue in the literature. After a certain number of cycles, fracture occurs due to the initiation and propagation of cracks in what constitutes structural fatigue [Eggeler et al. (2004)].

Most of the data available in the literature correspond to rotary bending experiments performed at high cycling frequencies [Miyazaki et al. (1999), Rahim et al. (2013), Pelton et al. (2013)]. Under these testing conditions, complex stress states and temperature effects associated with the exothermic–endothermic character of the involved phase transformations are introduced. This makes difficult to understand the role of the stress induced transformation on fatigue life. Also the strain rate is usually ignored when analyzing data obtained in different tests [Robertson et al. (2012)]. Although some authors performed experiments under uniaxial loading conditions, important aspects were not taken into account [Nayan et al. (2009), Kang et al. (2012)]. They include the localized nature of the stress induced transformation, the number of active transformation fronts, the maximum local temperature due to thermal effects associated with the first order martensitic transformation and the resulting maximum stresses and their impact on fatigue life. Therefore, there is a need of generating experimental information from simple tests performed under well-defined conditions.

With the purpose of clarifying one of the main aspects, i.e. the role of the stress induced martensitic transformation on the fatigue life of Ni-rich ultrafine grained NiTi superelastic wires, two types of fatigue tests have been analyzed in the present work. They will be referred to as cycling tests (CT) and pseudoelastic cycling (PC) in what follows. CT type of testing is performed by cycling in between the stress levels associated with the upper and lower plateau corresponding to the first cycle of a full pseudoelastic loop performed at the same temperature. By limiting the stress in this way it is expected that no evident stress induced transformations between the involved phases occur. CT type of cycling experiments have been performed in fully austenite, in fully stress induced martensite and at mid-plateau strain, which corresponds to a nearly half of the wire free length (length between grips). PC testing, on the contrary, involves forward–reverse B2 to B19' stress induced transformation (more details will be provided later in a specific section). Resulting fatigue lives for CT and PC testing are compared.

Additional important aspects related with fatigue life of NiTi wires are also considered. They refer to fretting fatigue effects in the grip–specimen contact region and to the relative importance of the crack initiation and crack propagation stages on the total fatigue life.

2. Material and experiments

In the present work, commercial ultrafine grained (40-50 nm) superelastic NiTi wires (Ti-50.9 at.% Ni) with a diameter of 0.5 mm (SAES Getters) have been characterized. Wires were received in the 'straight annealed' thermomechanical condition with a hard black oxide surface condition. The austenitic phase was stable at ambient temperature, with an A_f temperature of $-15\text{ }^\circ\text{C}$ for the fully annealed state according to manufacturer specification. A special gripping device was developed for the present work to minimize grip induced failures. The design of the device is based on the friction of a wire rolled on a cylinder. The diameter of cylinder was determined to be 50 mm in order to obtain a strain less than 1% for preventing martensitic transformation during mounting. Wire specimens with a total length of 140 mm were used. The free length between grips L_0 was set to 60 mm. Specimen deformation is given in terms of an apparent strain referred to as ϵ_{CH} (CH-crosshead) which is obtained by dividing the testing machine crosshead displacement (electromechanical testing machine), alternatively piston displacement (servohydraulic testing machine), by the free length between grips L_0 .

Cycling tests (CT) were performed at constant temperature equal to 37 °C using a MTS 810 universal servohydraulic machine equipped with a temperature chamber. Force measurements were performed with a 5 kN full-scale MTS load cell. Tests were conducted under crosshead displacement control at a frequency of 5 Hz. Cycling parameters are shown in Table 1. The strain amplitude was defined in such a way that the resulting stress amplitude remains confined between the upper and lower plateaus stress levels corresponding to the temperature of 37 °C. This can be appreciated in Fig. 1 where representative cycles are included for fully austenite (cycle A), fully stress induced martensite (cycle H) and for mid-plateau condition (cycle E). The resulting maximum applied stress and amplitude stress are also shown in Table 1 for each test. A full pseudoelastic cycle performed at a crosshead speed of 0.1 mm/min at the same temperature of 37 °C is included as a reference.

Pseudoelastic cycling (PC) was performed in a dual-column Instron 5567 electromechanical testing machine equipped with a temperature chamber Instron 3119 and instrumented with a 1 kN full-scale Instron 2525 load cell. Tests were conducted under crosshead displacement control at crosshead speed of 0.1 and 1 mm/min (details are given below). These experiments were performed at temperatures of 25 °C, 37 °C and 50 °C.

3. Results and discussion

3.1. Cycling tests

Fig. 1 shows the stress-strain values during the initial cycles of three experiments, superimposed on the quasistatic stress-strain curve of a complete superelastic cycle. Nine tests were performed and main parameters are shown in Table 1. In all cases the mean strain was configured in the first loading cycle. In all performed cycling tests a negligible hysteresis was observed.

In all the cases, the maximum stress remained below 600 MPa and the stress amplitudes under 89 MPa. This assured that no evident phase changes were induced during cycling. As can be seen from Table 1, specimens cycled in the fully austenite phase reached lives above 7×10^6 cycles without fracture. In the other two cases, specimens fractured at a finite number of cycles with fracture occurring in the area of contact with the grips.

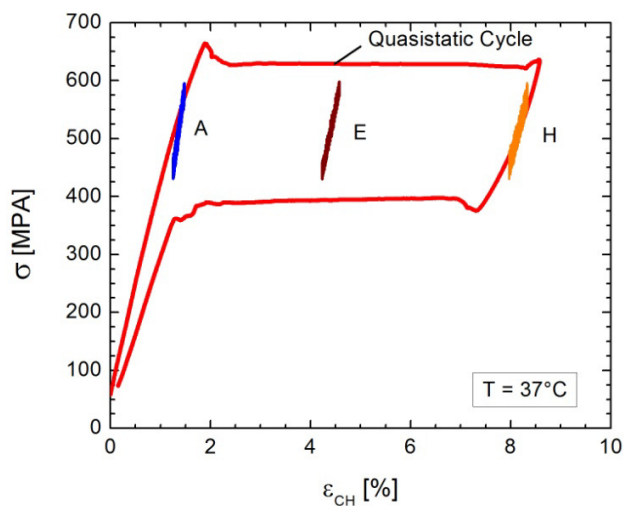


Fig. 1. Cyclic tests superimposed on a quasistatic reference pseudoelastic cycle performed at the same temperature. A: fully austenite; H: fully stress induced martensite; E: wire half-length transformed to martensite.

Table 1. Cycling test (CT) parameters and resulting fatigue lives for the three conditions considered.

Material States	Specimen	$\varepsilon_{\text{mean}}$ (%)	ε_a (%)	σ_{max} (MPa)	σ_a (MPa)	Number of cycles to fracture N_f
Austenite	A	1.80	0.10	587	89	> 10,000,000
	B	1.37	0.11	595	82	> 7,000,000
	C	1.46	0.09	581	74	> 10,000,000
Mid-plateau	D	4.91	0.18	581	76	2,513,480
	E	4.41	0.18	598	84	4,247,129
	F	4.48	0.14	599	83	967,558
Martensite	G	7.87	0.24	598	85	895,015
	H	8.15	0.19	596	83	932,956
	I	8.12	0.26	590	83	566,954

In comparison with results reported in the literature for similar type of CT experiments performed in NiTi superelastic tubes [Tabanlı et al. (1999)], the lives reported here are in all cases at least one order of magnitude higher. As an example, for CT cycling in the austenite phase, Tabanlı et al. (1999) reported a life of 185,000 cycles while in the present work the results of experiments A, B and C indicate a fatigue life above 7×10^6 cycles. However, it is important to remark that fatigue lives reported in Tabanlı et al. (1999) mostly correspond also to fractures occurring in the contact area between specimen and grips. This has occurred in our work even special precautions to reduce the chance of this type of failure were taken by a specific design of the gripping method.

The root cause of failure for the experiments performed in the present work has been analyzed by performing scanning electron microscopy (SEM) observations of the region close to the fracture surface, always occurring close to the incipient contact between specimen and grips cylinders. Surface marks compatible with a fretting wear process were identified in all the three tested conditions as can be appreciated in Fig. 2. Moreover, they are clearly related with the crack initiation location shown in Figs. 2(b) and (c). These findings are in line with previous observations reported by Qian et al. (2000).

The results discussed in the previous paragraph indicate that obtaining the true fatigue life of NiTi wires may be hindered by the presence of alternative damage initiation mechanisms like those shown here related with fretting. This is an important aspect that must also be adequately taken into account in technological applications. Careful design of wire gripping system is required in order to assure adequate fatigue life and this is an aspect deserving further research attention.

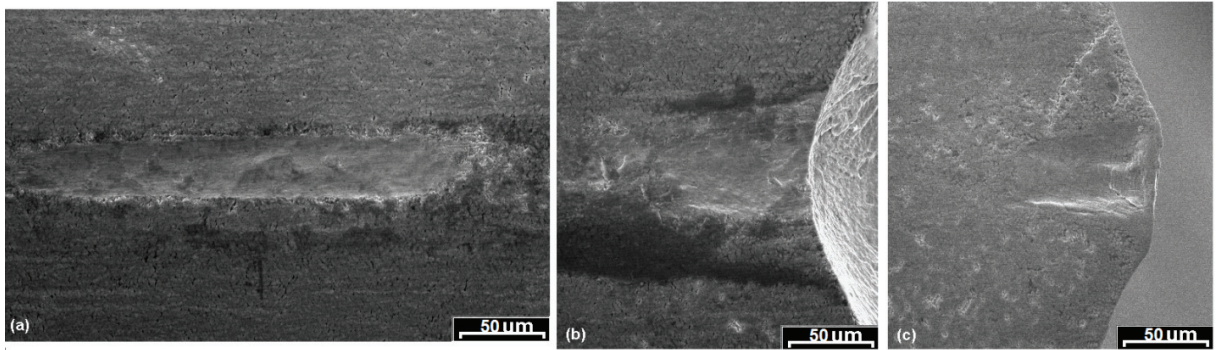


Fig. 2. Wire contact surface. (a) Austenite (no fracture); (b) partially stress induced martensite; (c) fully stress induced martensite. Loading direction is horizontal and fracture surface in plane in (b) and (c) is approximately normal to the page. Fretting marks on the lateral surface are related with fatigue crack initiation points.

A closer look at the conditions and results presented in Table 1 may suggest interpreting that fatigue life is correlated with mean strain value ϵ_{mean} . In effect, fatigue life decreased in going from experiments A, B, C to D, E, F and G, H, I that have been performed at increasing representative mean strain levels of 1.4%, 4.7% and 8.0%, respectively. However, some other important aspects must be taken into consideration for a correct analysis. The first concerns the localized character of the stress induced martensitic transformations exhibited by ultrafine grained NiTi wires subjected to uniform uniaxial tensile loading conditions [Olbricht et al. (2008), Soul and Yawny (2013)]. Due to that, the three conditions for the CT tests included in Table 1 differ only in the proportion of the B2 (austenite) and B19' (martensite) phases that are present (100% B2 for tests A, B and C; around 50% B2 / 50% B19' for tests D, E, F and 100% B19' for G, H and I). The individual phases are subjected to same stress variation in all cases and the associated strain ranges are determined by the corresponding elastic modulus. Therefore, it would be more appropriate rationalizing the decrease in fatigue life observed as depending on the proportion of martensite phase present at the specific condition, with the martensite phase exhibiting the lower resistance to fatigue cycling and with this resistance in turn depending on the absolute volume subjected to varying loads. Considering the limited amount of experimental information available, the previous assertion is considered rather speculative and further work is still required to shed more light on the question.

3.2. Pseudoelastic cycling

PC experiments were carefully designed in order to diminish the chance of specimen–grip interaction induced failures. This effect was expected to be even more life determining in the present case due to the high level of relative displacement between both elements associated to the transformation strain between B2 and B19' phases, close to 7%. The consideration of the localized character of stress induced transformation is also mandatory. PC experiments were therefore performed in two stages. In the first, the specimen was tensile stressed up to 5.65% strain, point A in Fig. 3(a), and then partially retransformed upon unloading to 4.06% strain, point B in the same figure. This sequence is represented by the black path $N = 0$ in Fig. 3(a). As it is well known from previous studies of the present authors, among others, the stress induced transformation in NiTi wires proceeds by the propagation of fronts that have been nucleated in the gripping area. Thus, it is usual to observe one or two transformation fronts sweeping the specimen towards the centre upon increasing the imposed displacement. In the present case, only one front was active. Starting from point B, continuous cycling in the range 4.06% to 5.65% strain was performed using a displacement rate of 0.1 mm/min. The first cycle is represented by the red cycle $N = 1$ in Fig. 3(a). The situation corresponds to approximately 10 mm of wire active length which defines what will be referred to in the next lines as the region of interest. Under this well controlled quasistatic conditions, a unique B2/B19' interface was kept moving forth and back with further cycling. In this way, thermal effects favouring the nucleation of additional interfaces out of the region of interest are avoided [Olbricht et al. (2008)].

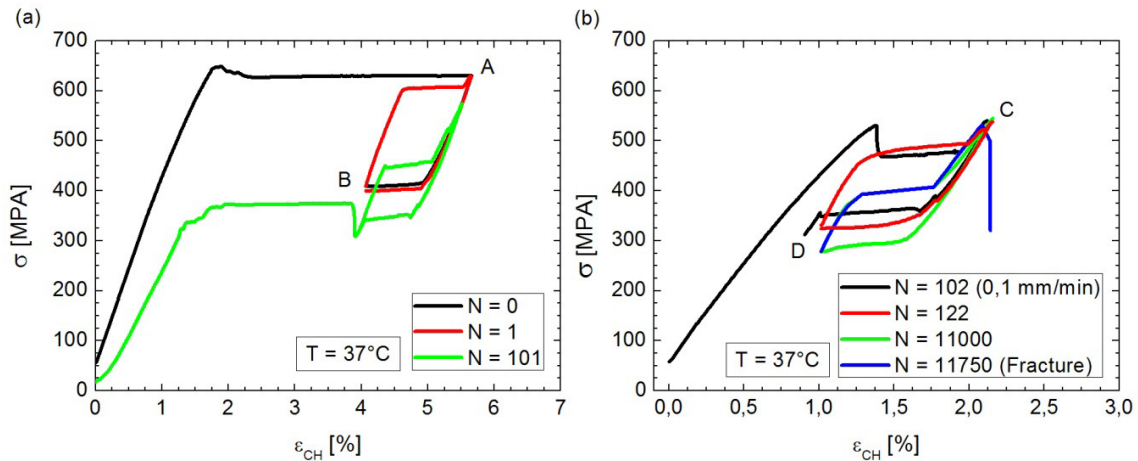


Fig.3. Pseudoelastic cycling (PC) experiment performed at 37 °C. (a) First stage performed at 0.1 mm / min corresponds to stabilization of the region of interest; (b) second stage performed at 1 mm/min until fracture.

A number of 101 cycles were performed in that way. The specimen was then completely unloaded before starting with the second stage of the test. The last quasistatic cycle and the final unloading path are represented in green as $N = 101$ in Fig. 3(a). It can be seen that as a consequence of the previous cycling, a decrease in the stress levels associated with the transformation plateaus in the region of interest is obtained. The magnitude of the decrease of the critical stress for the direct transformation becomes higher than the overstress necessary to nucleate a new transformation domain determined in Soul et al. (2013). Thus, it is expected now that a further loading will result in a transformation front nucleating inside the region of interest and also that the cycling speed could be safely increased in order to accelerate the fatigue process in that region. The second stage started with the path drawn in black colour denoted as $N = 102$ in Fig. 3(b) where, using a crosshead speed of 0.1 mm/min, the specimen was loaded up to point C and then unloaded down to point D. It can be seen that the stress-strain curve showed a response similar to cycle $N = 101$ except for the overstress peak at the onset of direct transformation. This peak corresponds to the nucleation of the mentioned transformation domain at the interface between the region on interest and the specimen. After reaching point D, crosshead displacement rate was increased to 1 mm/min and the specimen was cycled between 1.00% and 2.16% strain until fracture. The comparison of cycle $N = 122$ performed at 1 mm/min with cycle $N = 102$ performed at 0.1 mm/min illustrates the importance of the heat of transformation effects on the fatigue process. A widening of the hysteresis for cycle $N = 122$ is observed with an increase of 15 MPa over the stress level for the forward plateau and a decrease of 20 MPa for the reverse plateau. An increase in deformation rate thus alters the stress range and the maximum stress reached for given displacement limits and would then be expected to play a role in pseudoelastic fatigue life. This fact is usually ignored when analysing fatigue data obtained at different displacement rates or at the same rate using different strain amplitudes, e.g. Robertson et al. (2012) and references therein. For the PC experiment described in Fig. 3(b), the final rupture occurred at $N_f = 11,750$ cycles in the region of interest. This suggests that the here designed experiment can be considered successful in describing the true fatigue life of NiTi superelastic wires. The comparison of the fatigue life obtained in the PC experiment with the CT results presented in the previous section allows concluding on the decisive role played by the stress induced transformation in determining fatigue life. In this case, life was reduced to a level close to 2% of the minimum value reported in Table 1, corresponding to CT experiment performed in fully stress induced martensite.

In order to analyze the effect of stress on fatigue life, similar PC experiments were performed at 25 °C and 50 °C. By varying the temperature, the stress level is modified according to the Clausius-Clapeyron relationship which is close to 7 MPa/K for the material used here [Soul et al. (2013)]. Table 2 summarizes the experimental conditions and the fatigue lives N_f obtained for the three temperatures considered. As under the imposed strain limits, the maximum stress and amplitude were observed to vary along the cycling life, the values of σ_{\max} and σ_a reported in Table 2 were calculated by averaging the values recorded along the test. It can be seen that the reported fatigue lives differ less than 25%. Similarly to what has been observed for the PC test performed at 37 °C, fracture always occurred in the region of interest which confirms the appropriateness of the proposed method. No evident signs of fretting damage in the specimen–grip contact region have been observed in the case of PC cycling. This is understood in terms of reduced number of cycles to failure in comparison with lives reported in Table 1 for CT experiments.

Table 2. Pseudoelastic cycling (PC) parameters and resulting fatigue lives for the three temperatures considered.

Temperature (°C)	ε_a (%)	σ_{\max} (MPa)	σ_a (MPa)	Number of cycles to fracture N_f
25	1.16	518	199	13,597
37	1.16	542	126	11,750
50	1.16	587	88	14,636

3.3. Fracture surface analysis

An analysis of the fracture surface of specimens cycled in PC experiment at 37 °C was performed by SEM (Fig. 4). Four distinct regions could be identified and they are denoted by numbers from 1 to 4 in Fig. 4(a). Region 1 corresponds to the initial crack growth region with the initiation point indicated by the arrow at the bottom. Region 2 is characterized by the coexistence of fatigue-crack growth and ductile failure. Region 3 corresponds to the final rupture exhibiting complete ductile character. Region 4 corresponds to the shear lips delimiting the perimeter of the wire surface associated with the final fracture. Fig. 5 shows magnified views of the four mentioned zones. Crack initiation occurred on the surface as can be appreciated in Figs. 4 and 5(a), however no clear identification of the presence of a carbide or oxide particle as initiator could be performed. Fig. 5(b) allows identifying characteristic striation lines and, from their width, an average subcritical crack propagation rate $da/dN = 1 \mu\text{m}/\text{cycle}$ could be estimated. Taking into account that the final ductile fracture surface represents around 50% of the total fracture surface, 250 cycles would be required to advance the crack a distance of 250 μm . This represents only 2% of the total life $N_f = 11,750$ cycles. The present results indicate that, even when fatigue life has been drastically reduced compared with those observed under CT conditions, damage initiation is the dominant stage determining the lifetime in PC experiments. This observation is somehow contrary to what is usually observed in fatigue of conventional materials where the relative extension of the crack initiation stage diminishes as fatigue life decreases.

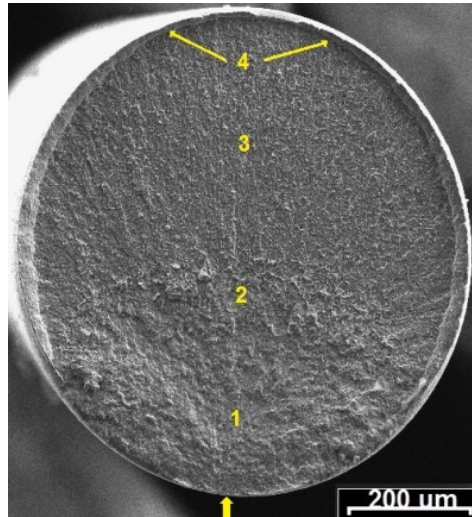


Fig. 4. SEM micrographs showing the characteristic regions identified on the fatigue fracture surface of NiTi superelastic wires subjected to PC experiments ($N_f = 11,750$). Region 1: damage initiation and initial crack propagation; Region 2: mixed crack propagation / ductile fracture; Region 3: final ductile fracture; Region 4: shear lips on the wire perimeter accompanying final fracture.

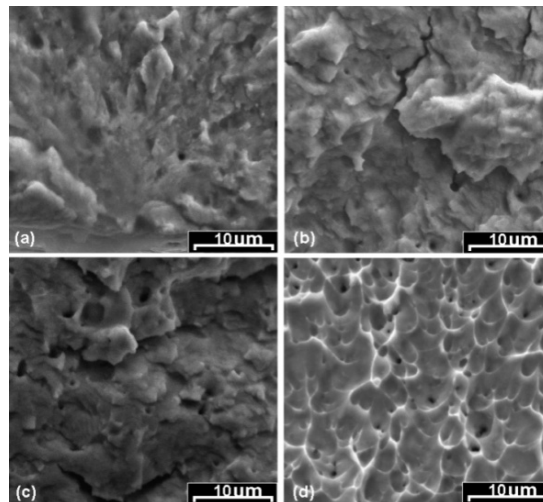


Fig. 5. SEM magnified micrographs corresponding to regions identified in Fig. 4 as (a) 1, (b) 2, (c) 3 and (d) 4, respectively.

4. Conclusion

As a general trend, results of constant state pull-pull fatigue tests showed higher lives for fully austenite samples, followed by partially martensitic. Finally the lowest life values were found for the fully martensitic samples. In comparison with pseudoelastic tests, obtained lives are in all cases at least two orders of magnitude higher. These results showed that the presence of the martensitic transformation constitutes a critical factor in reducing the fatigue life. Although the stress ranges applied to the pseudoelastic cycling suffered changes, they remained close to the applied stress in the fatigue test without phase change.

A process of fretting fatigue crack initiation was found in the cycling tests without phase changes. This process is less important in the pseudoelastic cycling as fatigue life is governed by the martensitic transformation.

The comparison of present results with those reported by other authors indicate that the experimental method to fix the samples in the tensile test plays a significant role if wires are considered.

Due to the nature of the martensitic transformation, thermal effects should be considered when studying the fatigue life of Ni-Ti alloys.

The analysis of the fracture surface indicated that under the cycling conditions used, the initiation step is the one that determines the lifetime of the sample.

Acknowledgments

The authors would like to acknowledge the financial support from CONICET, ANPCyT PICT 0898 – 2011 and SeCTyP UNCuyo and the technical assistance of Mr. P. Riquelme, Mr. A. C. Gómez Bastidas (CAB-CNEA) and Mr. M. Kalafatovich (INTEMA-CONICET).

References

- Dowling, N.E., Calhoun, C.A., Arcari, A., 2009. Mean stress effects in stress-life fatigue and the Walker equation. *Fatigue Fract. Eng. Mater. Struct.* 32, 163–179.
- Eggeler, G., Hornbogen, E., Yawny, A., Heckmann, A., Wagner, M., 2004. Structural and functional fatigue of NiTi shape memory alloys. *Mater. Sci. Eng. A* 378, 24–33.
- Kang, G., Kan, Q., Yu, C., Song, D., Liu, Y., 2012. Whole-life transformation ratchetting and fatigue of super-elastic NiTi Alloy under uniaxial stress-controlled cyclic loading. *Mater. Sci. Eng. A* 535, 228–234.
- Melton, K., Mercier, O., 1979. Fatigue of NITI thermoelastic martensites. *Acta Metall.* 27, 137–144.
- Miyazaki, S., Mizukoshi, K., Ueki, T., Sakuma, T., Liu, Y., 1999. Fatigue life of Ti – 50 at .% Ni and Ti – 40Ni – 10 Cu (at .%) shape memory alloy wires. *Mater. Sci. Eng. A* 273-275, 658–663.
- Nayan, N., Buravalla, V., Ramamurty, U., 2009. Effect of mechanical cycling on the stress–strain response of a martensitic Nitinol shape memory alloy. *Mater. Sci. Eng. A* 525, 60–67.
- Olbricht, J., Yawny, A., Condó, A.M., Lovey, F.C., Eggeler, G., 2008. The influence of temperature on the evolution of functional properties during pseudoelastic cycling of ultra fine grained NiTi. *Mater. Sci. Eng. A* 481-482, 142–145.
- Pelton, A.R., Fino-Decker, J., Vien, L., Bonsignore, C., Saffari, P., Launey, M., Mitchell, M.R., 2013. Rotary-bending fatigue characteristics of medical-grade Nitinol wire. *J. Mech. Behav. Biomed. Mater.* 27, 19–32.
- Proft, J.L., Melton, K., Duerig, T.W., 1989. Transformational cycling of Ni-Ti and Ni-Ti-Cu shape memory alloys, in "MRS International Meeting on Advanced Materials ". In: Doyama, M., Somiya, S., Chang, R. (Eds.), MRS, Tokyo, Japan, pp. 159–164.
- Pelton, A.R., DiCello, J., Miyazaki, S., 2000. Optimization of processing and properties of medical-grade Nitinol wire, International Conference on Shape Memory and Superelastic Technologies SMST-2000. Pacific Grove, CA, USA, pp. 361–374.
- Qian, L., Zhou, Z., Sun, Q., 2005. The role of phase transition in the fretting behavior of NiTi shape memory alloy. *Wear* 259, 309–318
- Rahim, M., Frenzel, J., Frotscher, M., Pfetzing-Micklich, J., Steegmüller, R., Wohlschlägel, M., Mughrabi, H., Eggeler, G., 2013. Impurity levels and fatigue lives of pseudoelastic NiTi shape memory alloys. *Acta Mater.* 61, 3667–3686.
- Robertson, S.W., Pelton, A.R., Ritchie, R.O., 2012. Mechanical fatigue and fracture of Nitinol. *Int. Mater. Rev.* 57, 1–36.
- Saburi, T., 1998. Ti-Ni shape memory alloys, in "Shape Memory Materials". In: Otsuka, K., Wayman, C.M. (Eds.). Cambridge University Press, Cambridge, UK, pp. 49–96.
- Soul, H., Yawny, A., 2013. Thermomechanical model for evaluation of the superelastic response of NiTi shape memory alloys under dynamic conditions. *Smart Mater. Struct.* 22.
- Tabanlı, R.M., Simha, N.K., Berg, B.T., 2001. Mean strain effects on the fatigue properties of superelastic NiTi. *Metall. Mater. Trans. A* 32, 1866–1869.
- Yawny, A., Sade, M., Eggeler, G., 2005. Pseudoelastic cycling of ultra-fine-grained NiTi shape-memory wires. *Int. J. Mater. Res. (Zeitschrift für Met.)* 96, 608–618.